

Evaluation of two and three fluid nozzle spray drying to prepare co-crystals of salicylic acid and caffeine with improved physicochemical properties

Article

Published Version

Creative Commons: Attribution 4.0 (CC-BY)

Open Access

Hibbard, T., Shankland, K. ORCID: <https://orcid.org/0000-0001-6566-0155> and Al-Obaidi, H. ORCID: <https://orcid.org/0000-0001-9735-0303> (2023) Evaluation of two and three fluid nozzle spray drying to prepare co-crystals of salicylic acid and caffeine with improved physicochemical properties. Journal of Drug Delivery Science and Technology, 89. 105073. ISSN 1773-2247 doi: 10.1016/j.jddst.2023.105073 Available at <https://centaur.reading.ac.uk/113737/>

It is advisable to refer to the publisher's version if you intend to cite from the work. See [Guidance on citing](#).

To link to this article DOI: <http://dx.doi.org/10.1016/j.jddst.2023.105073>

Publisher: Elsevier

All outputs in CentAUR are protected by Intellectual Property Rights law, including copyright law. Copyright and IPR is retained by the creators or other copyright holders. Terms and conditions for use of this material are defined in

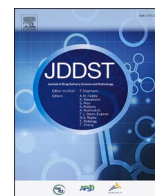
the [End User Agreement](#).

www.reading.ac.uk/centaur

CentAUR

Central Archive at the University of Reading

Reading's research outputs online



Evaluation of two and three fluid nozzle spray drying to prepare co-crystals of salicylic acid and caffeine with improved physicochemical properties

Thomas Hibbard, Kenneth Shankland, Hisham Al-Obaidi *

School of Pharmacy, University of Reading, Reading, RG6 6AD, UK

ARTICLE INFO

Keywords:

Co-crystals
Spray drying
Dissolution rate
Tablets
Caffeine
Salicylic acid

ABSTRACT

Formation of co-crystals using spray drying remains a challenging task due to the rapid nature of the process and the possible impact of solvents on the formation of the co-crystals. The purpose of this work was to generate co-crystals via two-fluid and three-fluid nozzle spray drying using the model system of salicylic acid and caffeine (SAL-CAF). The prepared co-crystal showed a strong tendency to form through spray drying, from a variety of feedstock compositions and through both two-fluid and three-fluid drying methods. Powder X-ray diffraction, Fourier - Transform infrared spectroscopy and differential scanning calorimetry were used to characterise the spray dried powders through comparison to the reported crystal structure and SAL-CAF formed through milling. All spray dried powders showed good agreement to the reported crystal structure but with an additional phase present, determined as the β -polymorph of caffeine. This additional phase was present at different proportions corresponding to the solvent, feedstock concentration and method used. For the three-fluid nozzle method, the feedstock composition was shown to have a large influence on the proportion of co-crystal in the final sample and all three-fluid nozzle samples showed reduced crystallinity compared to the two-fluid nozzle method. The spray dried co-crystals showed resistance to stress conditions over a period of four months and remained detectable following a tableting process. Spray drying is a suitable technique for the preparation of the SAL-CAF co-crystal and with further optimisation of process parameters may be equivalent or superior to milling.

1. Introduction

Co-crystals have become a successful crystal engineering strategy to formulate weakly ionisable, poorly soluble molecules for pharmaceutical applications [1]. New co-crystal forms of active pharmaceutical ingredients (APIs) are discovered and reported regularly, and now co-crystal formulations exist as licensed marketed products to be used clinically [2,3]. Of these products, Entresto® and Seglentis®, are drug-drug co-crystals where both components in the crystal structure have active pharmaceutical properties. The advantage of these new solid forms is that the resultant material will have modified physicochemical properties as well as synergistic pharmacodynamic effects. This may lead to a compound with enhanced absorption, therapeutic effect, and a reduction in the treatment burden for the patient. One drug-drug co-crystal which has been reported but not marketed is composed of salicylic acid (SAL) and caffeine (CAF), where CAF is known to have a synergistic effect for the management of pain [4]. SAL-CAF crystal structure has been reported previously and co-crystal forms of CAF are also known to display much improved stability through prevention of CAF hydration

[5,6]. Since SAL is a poorly soluble API, generation of a co-crystal with a highly soluble cofomer, such as CAF, may also be beneficial for enhancing solution properties.

Many production methods exist for the formation of co-crystals including solid state, solution, and hot-melt extrusion [1]. However, there are limitations associated with these approaches, including but not limited to, poor scalability, starting material or product degradation and reliance on large quantities of solvent. One approach which is highly scalable, adaptable, and non-destructive is spray drying. Spray drying has a common place in industry and has been shown to be able to generate co-crystals [7–12]. These studies indicated that spray drying was even able to generate co-crystals not readily formed through traditional slurry or reaction crystallisation methods [7], to an equivalent quality as milling methods [8] and in the presence of other excipients [9]. However, there is limited research with respect to the influence which process parameters have on the formation of a co-crystal during spray drying, which is essential when considering scale up preparation. As such we present a study using the model system of SAL-CAF where co-crystal preparation is assessed following systematic

* Corresponding author.

E-mail address: h.al-obaidi@reading.ac.uk (H. Al-Obaidi).

<https://doi.org/10.1016/j.jddst.2023.105073>

Received 3 August 2023; Received in revised form 3 October 2023; Accepted 14 October 2023

Available online 16 October 2023

1773-2247/© 2023 The Authors. Published by Elsevier B.V. This is an open access article under the CC BY license (<http://creativecommons.org/licenses/by/4.0/>).

variation of feedstock solvent composition, solute concentration and spray drying nozzle type.

Since SAL and CAF have different aqueous solubilities, a co-solvent feedstock with aqueous and organic phases is advantageous to ensure high solubility of both components. In this study, the solvent used as the organic phase was varied since the composition of the solvent system can have a large impact on which crystalline phases and what stoichiometric ratios will nucleate from a multicomponent system [13]. SAL-CAF preparation was also assessed using three-fluid nozzle spray drying, where SAL and CAF in separate feedstock solutions met at the point of atomisation which is an advantage considering the different solubilities [14]. It also allows the potential for higher feedstock concentrations which can limit solvent use, another variable which is evaluated in this study. There are no studies reporting the use of three-fluid nozzle spray drying to prepare co-crystals and as such demonstrating that co-crystals can be generated in this way would be advantageous for formulation development.

2. Material and methods

2.1. Materials

Salicylic acid (CAS: 69-72-7), caffeine (CAS: 58-08-2), α -Lactose monohydrate (CAS: 5989-81-1), Polyplasdone XL™, Magnesium Stearate (CAS: 557-04-0), acetone (CAS: 67-64-1, $\geq 99.8\%$) and ethanol (CAS: 64-17-5, $\geq 99.8\%$) were obtained from Sigma-Aldrich (Dorset, UK); propan-2-ol (CAS: 67-63-0, $>95\%$) was obtained from Fisher-Scientific Limited (Leicestershire, UK). All chemicals were used as received.

2.2. Preparation of Caffeine:Salicylic acid Co-crystal

2.2.1. Spray drying methods

Spray drying experiments were performed using a B-290 spray dryer (Büchi, Labortechnik AG Switzerland) operated in closed loop mode with a nitrogen atomising gas and nitrogen drying atmosphere. The aspirator was set to 100% generating a vacuum of -100 mbar and the atomising gas flow set to 660 L h^{-1} . An inlet temperature of 110°C was used for all experiments which were started when the outlet temperature stabilised at 60°C . A two-fluid nozzle (2-FN) or a three-fluid nozzle (3-FN) was used and feedstock was pumped at 5 mL min^{-1} . For the 3-FN, two feedstocks were pumped through the different nozzle channels simultaneously, using separate, synced pumps. Pumps were synced by measuring the time taken to pump a fixed volume of solvent. Feedstocks were prepared according to Table 1 and contained SAL and CAF in a 1:1 M ratio. For the 2-FN experiments, initially CAF and SAL were dissolved separately in aqueous and organic solvent phases respectively. Organic and aqueous phases were then combined and stirred using a magnetic stirrer to create a clear feedstock with the required final concentration. The organic solvent used, and total feedstock concentration were varied systematically in two Level factorial design. The experiments (exp) in Table 1 were repeated using 3-FN spray drying in which CAF (aqueous) was used as the internal feed and SAL (organic) as the external feed.

Table 1
Spray-drying methods for SAL-CAF formulations.

Experiment	Organic Solvent	Feedstock Concentration % w/v
1	Acetone	2
2	Acetone	0.5
3	Acetone	1
4	Ethanol	0.5
5	Ethanol	2
6	Ethanol	1
7	Propan-2-ol	2
8	Propan-2-ol	1
9	Propan-2-ol	0.5

2.2.2. Mechanochemical activation method (milling)

A milling method was used as a comparison to spray drying for the preparation of the SAL-CAF co-crystal as is a successful co-crystallisation method for CAF and SAL co-crystals alike [15–17]. An equimolar ratio of SAL and CAF were milled together with a small quantity of ethanol ($2 \mu\text{L mg}^{-1}$), using a Retsch MM 500 nano ball mill (Haan, Germany). 2.5 mm ball bearings were used in a 1:20 ball to starting material ratio and the sample was milled for 30 min at a frequency of 25 Hz.

2.3. Physicochemical analysis of spray dried samples

2.3.1. Powder X-ray diffraction (PXRD)

Transmission capillary PXRD data was collected for all spray dried formulations using a Bruker D8 Advance diffractometer (Massachusetts, USA) equipped with a monochromatic $\text{CuK}\alpha_1$ source. Samples were packed into a 0.7 mm borosilicate glass capillary then scanned in the range 4° – 45° 2θ using step size 0.0171° with a count time of 1.4 s per step.

Data for the starting materials were also collected using the same settings to be used as references. Full width half max (FWHM) values were calculated using EVA program (Bruker) for known SAL-CAF diffraction peaks as a comparison between spray drying methods. Phase Rietveld fit was performed using TOPAS for all spray dried samples compared to unit cell parameters corresponding to Cambridge Structural Database (CSD) structures: XOBAT01 and NIFWEE03. PXRD data for the tablet surface was collected using a Bruker D8 Advance diffractometer operating in a reflection geometry using the same collection settings as the transmission data collection.

2.3.2. Fourier -transform infrared spectroscopy (FTIR)

FTIR spectra were collected using a PerkinElmer 100 FTIR Spectrometer equipped with a diamond attenuated total reflectance (ATR) accessory (Shelton, Connecticut, USA). Transmission was recorded from an average of 16 scans over the range 650 – 4000 cm^{-1} with a resolution of 4 cm^{-1} .

2.3.3. Differential scanning calorimetry (DSC)

Melting point analysis was performed for all samples using a TA-Q2000 Differential Scanning Calorimetry (DSC) instrument (TA instruments, New Castle, USA). Samples were sealed into aluminium hermetic pans, allowed to equilibrate at 30°C then heated at $10^\circ\text{C min}^{-1}$ to 160°C . Pan lids were pierced to allow removal of residual solvents from the system during heating. TA Universal Analysis software was used to describe any thermal events. Melting point was calculated using onset temperature and fusion enthalpy through linear integration.

2.3.4. Compression testing

Tablets were produced using a direct compression method following sheer mixing of SAL-CAF, disintegrant and filler then coating with lubricant according to Table 2. Three tablet powders were made using the milled SAL-CAF and SAL-CAF from Exp 4 and 4a (representative 2-FN and 3-FN methods). SAL-CAF tablets were produced using a KBR press with a force of 5 tons for 1 min. Following compression, tablet surface properties were analysed using PXRD.

Table 2
Tablet composition SAL-CAF compression tests.

Component	% w/w (to 250 mg)
SAL-CAF (milled, 2-FN or 3-FN)	20
PolyPlasdone XL	3
α -lactose monohydrate	to 100
Magnesium Stearate	1

2.3.5. Stress conditions for stability studies

Spray dried powders from Exp 4, 5 and 6 from both 2-FN and 3-FN methods were stored in a sealed desiccator at 37 °C (± 1 °C) for four months. A reservoir containing a saturated solution of NaCl was added to the desiccator to generate an environment with 75% relative humidity. The humidity level was verified using a humidity probe. Samples were monitored for a total duration of four months then were analysed using PXRD and FTIR.

2.4. Data analysis

Statistical analysis was carried out using SPSS software (IBM SPSS version 27.0, SPSS Inc.). Data were compared with appropriate statistical test following visualisation and measurement of normality and variance. In each case, statistical significance was defined as $p < 0.05$ with significance levels: *** = $p < 0.001$, ** $p < 0.01$, * = $p < 0.05$ and NS = $p > 0.05$.

3. Results and discussion

3.1. Preparation of SD formulations

Spray dried samples containing SAL and CAF were prepared according to the method outlined in section 2.2. The collected yield was calculated for each sample as a percentage of the total solid dissolved in the feedstock. No significant differences were seen when comparing % yield between different solvents or concentrations of feedstock (ANOVA, $p > 0.05$). Therefore, a mean yield was calculated for all 2-FN and 3FN samples (Fig. 1).

The 2-FN method shows a significantly higher yield than the 3FN method at 58% compared to 27% respectively. The low yield from the 3-FN could be due to an incomplete drying process leading to deposition within the spray drying apparatus [18]. This is likely since a higher volume of feedstock was being pumped through the nozzle i.e. from two pumps operating at 5 mL min^{-1} compared to one pump. Optimisation of process parameters for the 3-FN method by increasing inlet temperature or decreasing pump rate could compensate for this difference and potentially increase the yield.

3.2. Characterisation of spray dried product

3.2.1. Confirmation of Co-crystal formation – PXRD and DSC

PXRD data confirms the formation of a co-crystal through all spray drying methods and from all solvent systems (Figs. S1 and S2). The low

angle diffraction peak at $\sim 6.7^\circ 2\theta$ and the absence of any starting material peaks in the spray dried samples are indicative of co-crystal formation (Fig. 2). In addition to this, DSC thermograms for all spray dried materials showed a single endothermic peak with an onset temperature corresponding to that reported for SAL-CAF (i.e. 138°C – 140°C). This endothermic peak corresponds to the crystalline melting point of a single-phase material, confirming the absence of any residual starting material (Fig. 3).

There is also evidence of co-crystal formation through the milling method. However, some SAL and CAF reference peaks are still present, seen most clearly at $12.17^\circ 2\theta$ for CAF and $10.99^\circ 2\theta$ and $17.27^\circ 2\theta$ for SAL (Fig. S3). This suggests that the milling method used has not completely transformed the starting materials to co-crystal. DSC confirmed that there was a mixture of co-crystal and starting material phases following milling at 25 Hz for 30 min. This is shown by an additional endothermic peak at $\sim 122^\circ\text{C}$ corresponding to the eutectic melt between SAL and CAF as reported by Lu et al. and shown experimentally through DSC analysis of a SAL + CAF physical mix (Fig. 4 and S4) [6]. Since there is no exothermic peak between the eutectic melt and the main endothermic melt it can be concluded that no recrystallisation has taken place. Therefore, the presence of physical mixture as seen on the PXRD between co-crystal and starting material phases is confirmed rather than co-crystal formation following eutectic melting during the DSC experiment. Additional PXRD peaks which are not explained by starting materials or co-crystal are also seen in the milled product which are discussed in section 3.2.2.

3.2.2. Comparison of Co-crystal with reported crystal structure

PXRD patterns also show good agreement with XOBCT01 [6] simulated powder pattern as generated by Mercury program [19] (Fig. 2). However, for all samples, including milled, there is additional diffraction seen at $\sim 11.9^\circ 2\theta$, $26.5^\circ 2\theta$ and $27^\circ 2\theta$ which is not explained by SAL-CAF or the corresponding starting material structures (Fig. 5). Following Rietveld refinement against reported crystal structures, it was determined that the peaks seen in spray dried and milled powders are clearly caused by the presence of the β -polymorph of CAF (Fig. 5, S5), known to be formed through dehydration of caffeine monohydrate [20, 21] and mechanochemical activation of anhydrous caffeine [22]. It is conceivable that during spray drying, due to feedstocks containing a mixture of aqueous and organic solvents, CAF could initially precipitate as the hydrate form then immediately dehydrate to the β -polymorph within the drying chamber. In addition, it has been shown that when a droplet formed of organic and aqueous components is dried, the evaporation of the organic phase can lead to rapid condensation of water

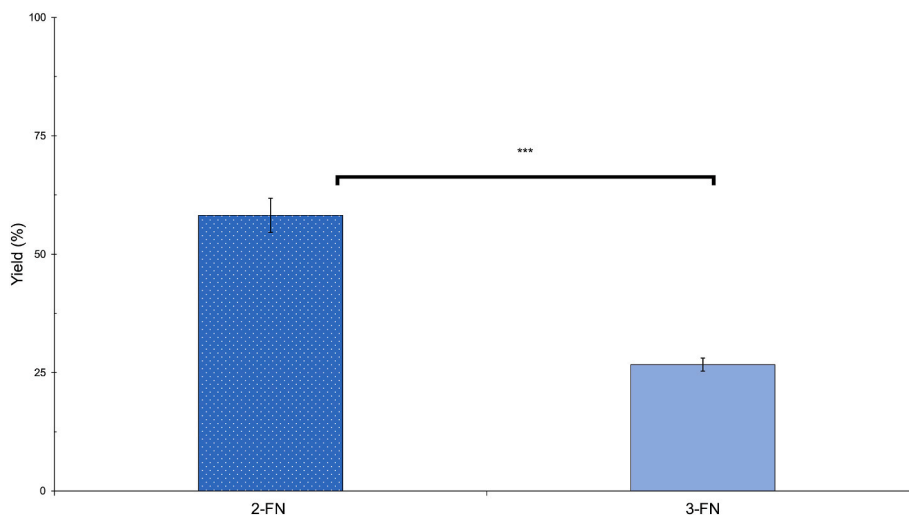
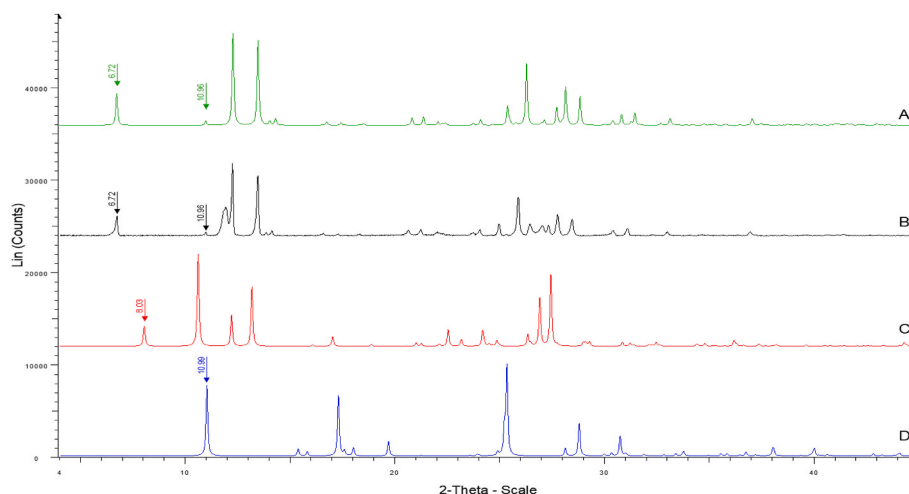


Fig. 1. Spray drying yields for two-fluid nozzle compared to three-fluid nozzle expressed as a mean of all experiments $n = 9$, $p < 0.001$.



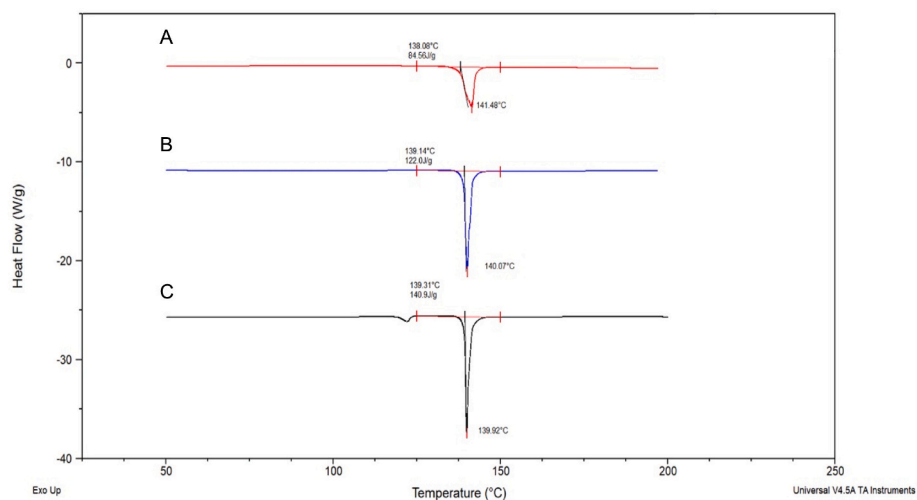


Fig. 4. DSC data for SAL-CAF co-crystal prepared through 3-FN (red) and 2-FN (blue) spray drying compared to milled SAL-CAF from milled method (black). The eutectic melt of salicylic acid and caffeine is seen at $\sim 122^\circ\text{C}$ in the milled sample. (For interpretation of the references to colour in this figure legend, the reader is referred to the Web version of this article.)

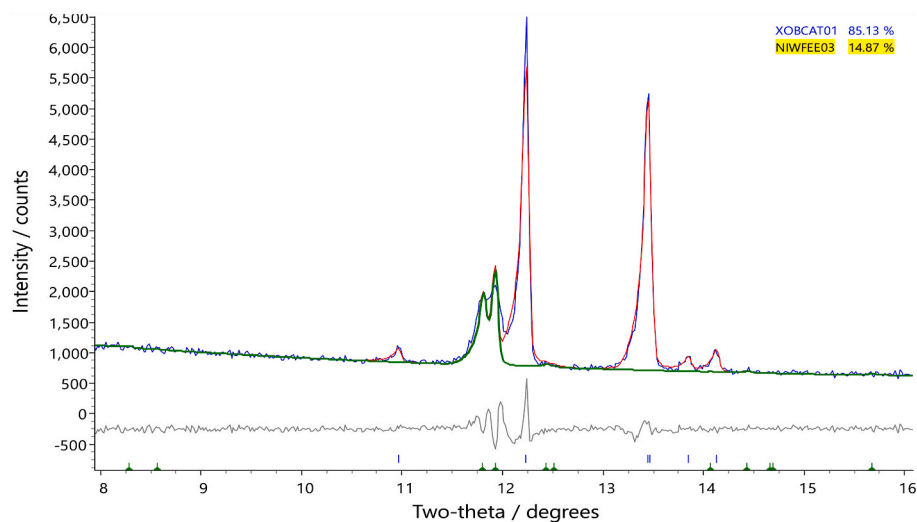


Fig. 5. Two-phase Rietveld fit of SAL-CAF Exp 4 using the structures corresponding to CSD redcodes XOBCAT01 (SAL-CAF co-crystal) and NIWFEE03 (CAF β -polymorph), shown in the range $8\text{--}16^\circ 2\theta$. PXRD data (blue line), the overall fit of co-crystal to the data (red line) and the contribution of the caffeine β -polymorph to the fit (green line) is displayed. Blue tick marks indicate the position of reflections associated with co-crystal phase, whilst green tick marks indicate the position of reflection associated with caffeine β -polymorph. The two observed reflections below $12^\circ 2\theta$ are explained by the presence of the caffeine β -polymorph. (For interpretation of the references to colour in this figure legend, the reader is referred to the Web version of this article.)

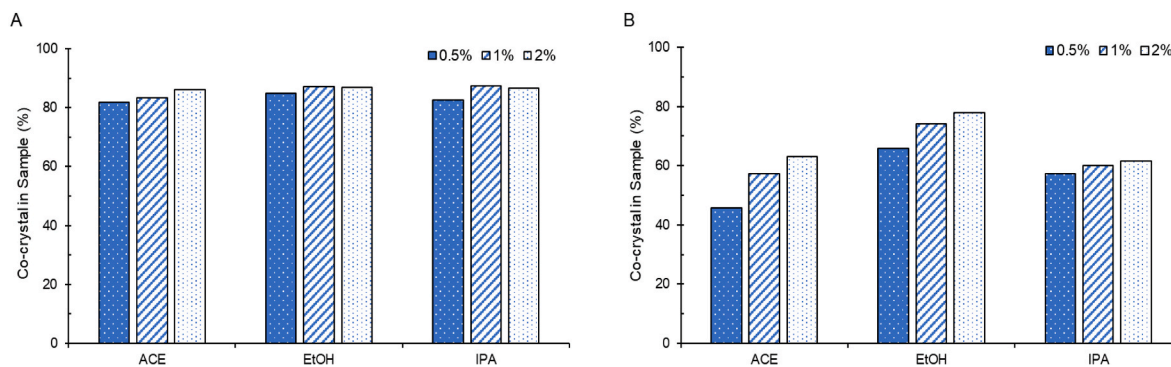


Fig. 6. Proportion of co-crystal phase present in spray dried samples as a ratio to the additional β -caffeine polymorph phase for A) two-fluid nozzle B) three-fluid nozzle.

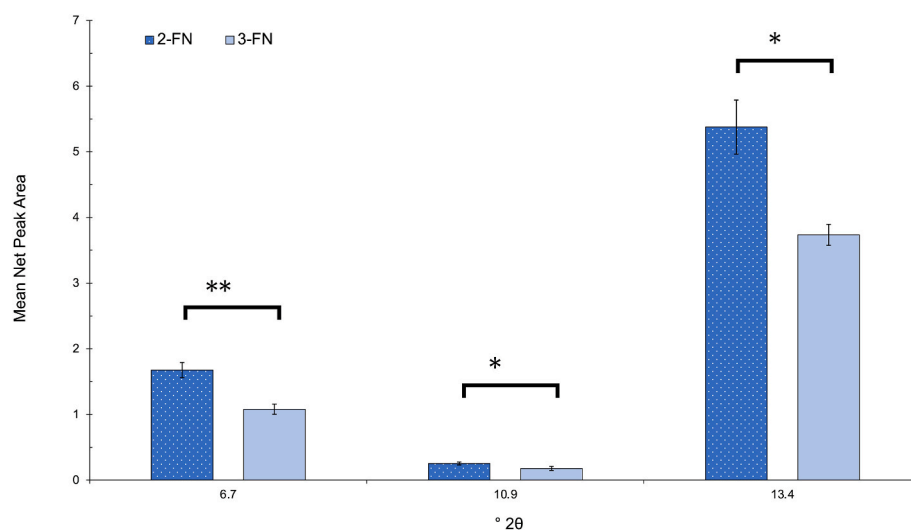


Fig. 7. Mean net peak area comparing 2-FN to 3-FN SAL-CAF across three co-crystal diffraction peaks.

the PXRD data which indicates that 3-FN spray drying gives a co-crystal with a lower degree of crystallinity to 2-FN spray drying (Table 3). Again, all spray drying products, show a lower enthalpy of fusion than the milled product although the difference between 2-FN and 3-FN is greater than between milled and 2-FN. These data confirm that in terms of crystallinity: milled > 2-FN > 3-FN.

3.2.4. Analysis of intermolecular interactions (FTIR)

Considering the FTIR data for spray dried samples, there is only slight change in the carbonyl region absorption bands compared to the CAF and SAL references (Fig. 8). The absorption bands are a composite of the reference bands at $\sim 1690\text{ cm}^{-1}$, $\sim 1655\text{ cm}^{-1}$, $\sim 1640\text{ cm}^{-1}$ and $\sim 1600\text{ cm}^{-1}$ for CAF, SAL, CAF and SAL respectively. The $\sim 1655\text{ cm}^{-1}$ and $\sim 1640\text{ cm}^{-1}$ bands overlap and so exist as a single broad absorbance in the product.

The formation of a co-crystal, rather than a salt, is supported through these data since during salt formation the carboxylic acid stretching

frequency is likely to move to a higher frequency. For example, Cook et al. showed that a series of CAF salts all showed carbonyl absorption bands at a higher frequency $\sim 1720\text{ cm}^{-1}$ and $\sim 1670\text{ cm}^{-1}$ compared to the free base reference which displays absorption at 1698 cm^{-1} and 1656 cm^{-1} [24]. There is a red shift present for the CAF component of the carbonyl region in all spray dried materials from $\sim 1652\text{ cm}^{-1}$ to $\sim 1657\text{ cm}^{-1}$ but this value is smaller than the reported red shift following the formation of CAF salts (to $\sim 1670\text{ cm}^{-1}$ [24]). The reduced red shift can be attributed to the formation of hydrogen bonds rather than ionic bonds between SAL and CAF. There is good agreement between the spectra for the 2-FN, 3-FN and milled product confirming the formation of a uniform product through all spray drying methods despite additional phases identified through PXRD analysis.

3.3. Physical properties of spray dried product

3.3.1. Humidity testing

PXRD and FTIR analysis of the samples stored in a high humidity environment for four months show no differences compared to references spectra taken prior to storage (Figs. S6, S7, S8).

PXRD shows the same peak positionings with no additional peaks corresponding to references seen. If hydration of the co-crystal had occurred there could have been a change to overall crystal structure arrangement which would have been seen through changes to the diffraction peaks. If there had been water sorption into the sample without changes to the crystal structure, FTIR would show additional peaks in the $3600\text{--}2800\text{ cm}^{-1}$ region. However, there is no evidence for this as shown by Figs. S6 and S7. In addition to these observations, the additional diffraction peaks associated with the CAF β -polymorph are still present in the samples following storage at high humidity.

3.3.2. Tablet compression testing

PXRD analysis following the tableting process reveals the presence of co-crystal and α -Lactose monohydrate on the surface of the 2-FN, 3-FN and milled co-crystal tablets. This confirms the sheer and tumble mixing processes were able to achieve a good mixture of co-crystal and excipients prior to compression, as seen by the presence of both main crystalline components on the tablet surface (Fig. S9). Physical stability of the co-crystal is also confirmed by the clear presence of key co-crystal reference peaks for 2-FN, 3-FN and milled tablets e.g. at $6.86^\circ 2\theta$.

There appears to be some shifting of peaks when comparing the diffraction patterns of the three tablets (Fig. 9). All peaks for the 2-FN and 3-FN tablets are shifted higher than the milled tablet by approximately $0.05^\circ 2\theta$ and $0.1^\circ 2\theta$ respectively. This could be due to the force

Table 3
DSC data for SAL-CAF samples.

Solvent	Nozzle Type	Feedstock Concentration (%)	Peak Onset ($^\circ\text{C}$)	ΔH_{fus} (J g^{-1})	Mean ΔH_{fus} (σ)
ACE	2-FN	0.5	139.5	103.4	109.7 (8.22)
		1	140.6	106.7	
		2	139.6	119.0	
	3-FN	0.5	138.3	56.4	64.6 (7.39)
		1	138.6	70.7	
		2	138.5	66.8	
EtOH	2-FN	0.5	139.1	124.1	118.0 (5.37)
		1	139.6	115.9	
		2	139.2	114.0	
	3-FN	0.5	138.1	86.6	92.0 (4.87)
		1	139.2	93.2	
		2	139.2	96.1	
IPA	2-FN	0.5	139.5	106.5	115.2 (8.17)
		1	139.3	122.7	
		2	139.2	116.5	
	3-FN	0.5	138.5	73.9	78.4 (3.91)
		1	138.6	81.2	
		2	138.8	80.0	
Milled SAL-CAF	n/a	n/a	139.3	140.9	140.9

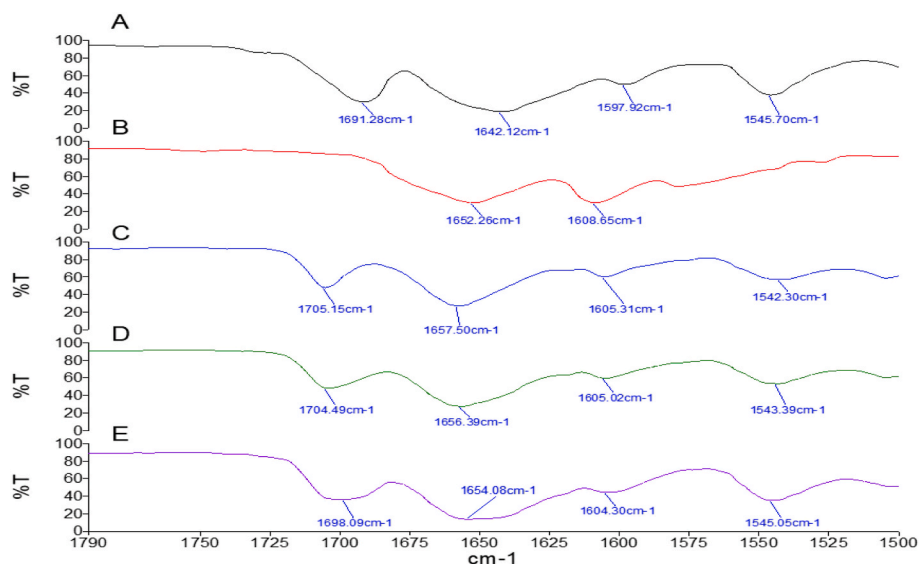


Fig. 8. FTIR data comparing A) CAF (black), B) SAL (red), C) SAL-CAF milled (blue), D) SAL-CAF 2-FN (green), E) SAL-CAF 3-FN (purple). (For interpretation of the references to colour in this figure legend, the reader is referred to the Web version of this article.)

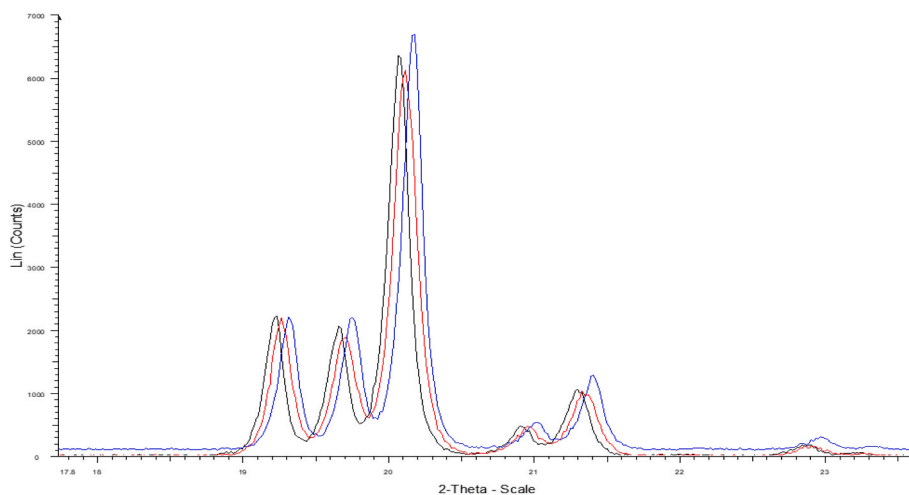


Fig. 9. Section of PXRD data showing α -lactose monohydrate peaks ($\sim 19^\circ 2\theta$ to $\sim 21.5^\circ 2\theta$) and co-crystal peaks ($\sim 23^\circ 2\theta$).

exerted on the crystal lattices during the compression process, causing a slight plastic deformation for each sample. Further experimentation to quantify how tableting processing parameters influence this is required.

4. Conclusions

The co-crystal of salicylic acid and caffeine has been prepared via a series of spray drying methods. SAL-CAF was successfully prepared regardless of the solvent systems, feedstock concentration or nozzle type although all spray drying methods showed the inclusion of phases separate to the co-crystal. The consistency in the product produced through these spray drying methods highlights the suitability of the SAL-CAF system for studying co-crystal formation in spray drying. Further work to optimise the process parameters is required to produce a pure co-crystal product. Additional phases were also seen in the equivalent milling method. All spray dried powders showed X-ray diffraction patterns associated with SAL-CAF co-crystal and a crystalline melt in agreement with previously reported values. The three-fluid spray drying method, where SAL and CAF combine in the nozzle from separate feedstocks also successfully prepared the co-crystal although to a lower crystallinity and higher proportions of additional phases than the

corresponding two-fluid spray drying method. Spray dried co-crystal powders showed stability following storage at elevated temperature and humidity and during an initial direct compression tableting method. Further studies to increase the yield of the three-fluid nozzle formulations and assess the dissolution properties of tablets containing the spray dried co-crystal powders are required.

CRediT author statement

TH: conceptualisation, investigation, methodology, writing – original draft, review & editing. KS: writing – original draft, review & editing; HAO: conceptualisation, investigation, methodology, project administration, writing – original draft, review & editing;

Declaration of competing interest

The authors declare that they have no known competing financial interests or personal relationships that could have appeared to influence the work reported in this paper.

Data availability

Data will be made available on request.

Appendix A. Supplementary data

Supplementary data to this article can be found online at <https://doi.org/10.1016/j.jddst.2023.105073>.

References

- [1] M. Karimi-Jafari, L. Padrela, G.M. Walker, D.M. Croker, Creating cocrystals: a review of pharmaceutical cocrystal preparation routes and applications, *Cryst. Growth Des.* 18 (10) (2018) 6370–6387.
- [2] A. Port, C. Almansa, R. Enrech, M. Bordas, C.R. Plata-Salamán, Differential solution behavior of the new API-API Co-crystal of tramadol-celecoxib (CTC) versus its constituents and their combination, *Cryst. Growth Des.* 19 (6) (2019) 3172–3182.
- [3] O.N. Kavanagh, D.M. Croker, G.M. Walker, M.J. Zaworotko, Pharmaceutical cocrystals: from serendipity to design to application, *Drug Discov. Today* 24 (3) (2019) 796–804.
- [4] G. Castañeda-Hernández, M.S. Castillo-Méndez, F.J. López-Muñoz, V. Granados-Soto, F.J. Flores-Murrieta, Potentiation by caffeine of the analgesic effect of aspirin in the pain-induced functional impairment model in the rat, *Can. J. Physiol. Pharmacol.* 72 (10) (1994) 1127–1131.
- [5] A.V. Trask, W.D.S. Motherwell, W. Jones, Pharmaceutical cocrystallization: engineering a remedy for caffeine hydration, *Cryst. Growth Des.* 5 (3) (2005) 1013–1021.
- [6] E. Lu, N. Rodríguez-Hornedo, R. Suryanarayanan, A rapid thermal method for cocrystal screening, *CrystEngComm* 10 (6) (2008) 665–668.
- [7] A. Alhalaweh, W. Kaialy, G. Buckton, H. Gill, A. Nokhodchi, S.P. Velaga, Theophylline cocrystals prepared by spray drying: physicochemical properties and aerosolization performance, *AAPS PharmSciTech* 14 (1) (2013) 265–276.
- [8] S.P. Patil, S.R. Modi, A.K. Bansal, Generation of 1:1 Carbamazepine:Nicotinamide cocrystals by spray drying, *Eur. J. Pharmaceut. Sci.* 62 (2014) 251–257.
- [9] D. Walsh, D.R. Serrano, Z.A. Worku, A.M. Madi, P. O'Connell, B. Twamley, et al., Engineering of pharmaceutical cocrystals in an excipient matrix: spray drying versus hot melt extrusion, *Int. J. Pharm.* 551 (1) (2018) 241–256.
- [10] M. Urano, M. Kitahara, K. Kishi, E. Goto, T. Tagami, T. Fukami, et al., Physical characteristics of cilostazol-hydroxybenzoic acid cocrystals prepared using a spray drying method, *Crystals* 10 (4) (2020) 313.
- [11] L.H. do Amaral, F.A. do Carmo, M.I. Amaro, V.P. de Sousa, L.C.R.P. da Silva, G. S. de Almeida, et al., Development and characterization of dapsone cocrystal prepared by scalable production methods, *AAPS PharmSciTech* 19 (6) (2018) 2687–2699.
- [12] J. Weng, S.N. Wong, X. Xu, B. Xuan, C. Wang, R. Chen, et al., Cocrystal engineering of itraconazole with suberic acid via rotary evaporation and spray drying, *Cryst. Growth Des.* 19 (5) (2019) 2736–2745.
- [13] T. Leyssens, G. Springuel, R. Montis, N. Candoni, S. Veessler, Importance of solvent selection for stoichiometrically diverse cocrystal systems: caffeine/maleic acid 1:1 and 2:1 cocrystals, *Cryst. Growth Des.* 12 (3) (2012) 1520–1530.
- [14] S. Focaroli, G. Jiang, P. O'Connell, J.V. Fahy, A.M. Healy, The use of a three-fluid atomising nozzle in the production of spray-dried theophylline/salbutamol sulphate powders intended for pulmonary delivery, *Pharmaceutics* 12 (11) (2020).
- [15] S. Latif, N. Abbas, A. Hussain, M.S. Arshad, N.I. Bukhari, H. Afzal, et al., Development of paracetamol-caffeine co-crystals to improve compressional, formulation and in vivo performance, *Drug Dev. Ind. Pharm.* 44 (7) (2018) 1099–1108.
- [16] S. Korde, S. Pagire, H. Pan, C. Seaton, A. Kelly, Y. Chen, et al., Continuous manufacturing of cocrystals using solid state shear milling technology, *Cryst. Growth Des.* 18 (4) (2018) 2297–2304.
- [17] F. Fischer, M. Joester, K. Rademann, F. Emmerling, Survival of the fittest: competitive Co-crystal reactions in the ball mill, *Chem. Eur. J.* 21 (42) (2015) 14969–14974.
- [18] M. Maury, K. Murphy, S. Kumar, L. Shi, G. Lee, Effects of process variables on the powder yield of spray-dried trehalose on a laboratory spray-dryer, *Eur. J. Pharm. Biopharm.* 59 (3) (2005) 565–573.
- [19] C.F. Macrae, I. Sovago, S.J. Cottrell, P.T. Galek, P. McCabe, E. Pidcock, et al., Mercury 4.0: from visualization to analysis, design and prediction, *J. Appl. Crystallogr.* 53 (1) (2020) 226–235.
- [20] C.W. Lehmann, F. Stowasser, The crystal structure of anhydrous β -caffeine as determined from X-ray powder-diffraction data, *Chem. Eur. J.* 13 (10) (2007) 2908–2911.
- [21] M.C. Allan, B. Owens, L.J. Mauer, Relative humidity–temperature transition boundaries for anhydrous β -caffeine and caffeine hydrate crystalline forms, *J. Food Sci.* 85 (6) (2020) 1815–1826.
- [22] J. Pirttimäki, E. Laine, J. Ketolainen, P. Paronen, Effects of grinding and compression on crystal structure of anhydrous caffeine, *Int. J. Pharm.* 95 (1) (1993) 93–99.
- [23] F. Gregson, M. Ordoubadi, R. Miles, A. Haddrell, D. Barona, D. Lewis, et al., Studies of competing evaporation rates of multiple volatile components from a single binary-component aerosol droplet, *Phys. Chem. Chem. Phys.* 21 (19) (2019) 9709–9719.
- [24] D. Cook, Z.R. Regnier, The infrared spectra of caffeine salts, *Can. J. Chem.* 45 (23) (1967) 2895–2897.